Magnetopiezoelectric effect and magnetocapacitance in $SmFe_3(BO_3)_4$

T. N. Gaydamak,[1] I. A. Gudim,[2] G. A. Zvyagina,[1] I. V. Bilych,[1] N. G. Burma,[1] K. R. Zhekov,[1] and V. D. Fil[1,*]

[1]*B. I. Verkin Institute for Low Temperature Physics and Engineering of the National Academy of Sciences of Ukraine, Lenin Ave., 47, Kharkov 61103, Ukraine*

[2]*L. V. Kirensky Institute for Physics, Siberian Branch of the Russian Academy of Sciences, Krasnoyarsk 660036, Russia*

(Received 22 June 2015; revised manuscript received 9 November 2015; published 21 December 2015)

A giant magnetopiezoelectric effect has been revealed in samarium ferroborate. The effective piezomodulus is increased more than twice in the antiferromagnetic phase and it is reduced by a high magnetic field. The nature of the effect is in the joint contribution of both magnetoelectric and magnetoelastic interactions. The evolution of this contribution in the magnetic field is caused by the growth of the magnetic energy including the spin reorientation. Additional data concerning the behavior of the high-frequency magnetocapacitance have been obtained. The parameters of magnetoelectric and magnetoelastic couplings and the magnetic anisotropy constant in the basal plane have been determined.

DOI: 10.1103/PhysRevB.92.214428 PACS number(s): 75.85.+t, 77.65.−j

I. INTRODUCTION

Rare-earth ferroborates [with the general formula $RFe_3(BO_3)_4$, where R stands for a rare-earth element] belong to the family of ferroelectromagnetics (multiferroics). These materials combine the properties of magnetically ordered and ferroelectric media. Following the terminology proposed in Ref. [1], they can be defined as type-II multiferroics, the materials in which the antiferromagnetic ordering is accompanied by the onset of an improper ferroelectricity. The interest in the study of ferroelectromagnetics in general and ferroborates in particular is caused by the prospect of their practical application [2], as well as by the wide range of various physical effects there. Up to now, a remarkable amount of information concerning their structure, magnetic, dielectric, magnetoelastic, and magneto-optical parameters has been already accumulated, and has been partially reviewed in Refs. [3,4].

Apparently, the greatest interest is in the study of the specific for ferroelectromagnetics "crossing" effects—the influence of the magnetic variables on the ferroelectric characteristics and vice versa. In particular, in some ferroborates, the spontaneous polarization caused by antiferromagnetic ordering and the one induced by the magnetic field have been detected [4]. The intensity of the latter is especially manifested in compounds that are "easy plane"-like antiferromagnetically ordered. First of all, this is related to samarium and neodymium compounds. Magnetodielectrical anomalies (the magnetocapacitance), i.e., the growth of the effective permittivity in an antiferromagnetic phase and its reduction to the value inherent in the paraelectric phase in a magnetic field, are closely associated to these phenomena. A giant magnetodielectric effect (∼100%) was revealed in the low-frequency characteristics of $SmFe_3(BO_3)_4$ (Ref. [5]) and $HoFe_3(BO_3)_4$ (Ref. [6]) single crystals. At the same time in the neodymium compound the magnetocapacitance is much smaller [4].

The crystal structure of ferroborates belongs to the noncentrosymmetric piezoactive class 32, similar to the well-studied α quartz [7]. However, the attention of the physics community to the piezoelectric characteristics of ferroborates was not so high until recently. There is only one experimental work [8] known to us in which by measuring the polarization charge arising under the static loading, the piezoelectric modulus (e_{11}) of $GdFe_3(BO_3)_4$ was evaluated at room temperature. According to those measurements, the piezoelectric modulus became nearly two times less than the one of the α quartz. This is why this compound was classified as a weak piezoelectric. It was incorrect to extrapolate that conclusion to the whole ferroborate family without additional experiments, and we have tried to fill this gap in knowledge. In our paper [9], the piezoelectric moduli (PM) of single crystals of $SmFe_3(BO_3)_4$ and $NdFe_3(BO_3)_4$ were evaluated using the acoustic method. It was found that in those compounds the value of the modulus e_{11} in the paraelectric phase (∼1.4 C/m^2) was almost an order of magnitude higher than that of the α quartz, and, therefore, such compounds may be recommended for technical applications.

The choice of compounds studied in Ref. [9] was not accidental. From general considerations, it could be assumed that phenomena like the magnetocapacitance can be observed in the piezoelectric response also. It appeared that the samarium compound demonstrates a giant magnetopiezoelectric effect—the effective PM is increased more than twice in the antiferromagnetic phase and it is suppressed by a magnetic field.

In addition, we have extended the measurements of the dielectric constant to a higher-frequency range (∼55 MHz) than in Ref. [5]. The magnetodielectric effect has been observed at these frequencies also. These measurements permit to estimate quantitatively the parameters of magnetoelectric and magnetoelastic couplings and to determine the effective constant of the easy-plane anisotropy.

II. EXPERIMENTAL TECHNIQUE AND THE RESULTS

$SmFe_3(BO_3)_4$ and $NdFe_3(BO_3)_4$ single crystals were grown by the method described in Ref. [10]. Samples were x-ray oriented and had typical sizes of nearly 2 mm.

All measurements were performed in a pulse (time of flight) regime at frequencies ∼55 MHz. The details of the measuring setup were described in Ref. [11]. Below, we describe in

*fil@ilt.kharkov.ua

more details some features of our experiments and the results obtained.

p experiment. The nonresonant acoustoelectric transformation is investigated. In one of the faces of the sample oriented in the piezoactive direction (in our case it was perpendicular to the face, i.e., oriented along the **x** axis) the high-frequency longitudinal deformation is exited (introduced via a delay line). It creates two normal modes: the acoustic wave, renormalized by the piezoelectric interaction, and the polarization one (some type of a "retarded potential") [12]. The electrical responses associated with these signals are registered by an electrode on the opposite face of the sample. In the time of flight experiment, we have two separated in time components. The fast electromagnetic component appears almost instantly in the relevant time scale. The slow component arrives at the receiving interface after a time of sound delay (nearly 0.25 μsec for our samples). One can estimate the magnitude of the fast component using simple "radio technical" considerations. There are many arguments (for example, the border conditions) that in the absence of an external electric field the induction in a sample is $\mathbf{D} = 0$. In the case of piezoelectrics (and ferroelectrics), it leads to the equation $\varepsilon_{xx}\frac{\partial\varphi_{in}}{\partial x} + 4\pi e_{11}\frac{\partial u_x}{\partial x} = 0$, see Ref. [13] ($\varphi_{in}$ is the electric potential at the exciting interface created by the elastic displacement, u_x is the amplitude of this displacement, and e_{11} is the piezomodulus). Integrating this equation results in the potential $\varphi_{in} = -\frac{4\pi e_{11}}{\varepsilon_{xx}}u_x$. This potential via the capacity formed by the sample (~0.2–0.5 pF), is transmitted to a receiving contact loaded onto the coaxial feeder. Since the input impedance of the matched receiving feeder differs a little from the wave resistance, $R_0 = 50$ Ohm, for our frequencies we deal with the differentiating circuit. Its transfer coefficient is proportional to the time constant τ ($\tau = R_0\varepsilon C_1$, C_1 is the geometric factor) and therefore to the permittivity. Thus the dependence of the potential registered by the receiver on ε is dropped out, and the amplitude of the fast signal reflects the behavior of only PM, or the polarization created by the sound wave. Below, all the results concerning the behavior of e_{11} are obtained by using the fast component (later called the p response). The amplitude of the slow component is of an order of magnitude comparable with the amplitude of the fast component. Its value is determined by the balance between the electromagnetic energy supplied to the interface and the rate of its scattering on the input impedance of the receiving system. As a result, the amplitude of the slow mode reflects the behavior of both PM and ε. It is also affected by the sound absorption and reflection coefficient of the receiving interface. For these reasons, an analysis of the behavior of the slow component was not carried out.

ε experiment. The sample under investigation is placed between the capacitor plates; the capacitor is used as a capacitive coupling element between the input and output feeders. Basically, this configuration resembles the ones discussed above. The difference is that in this case the potential on the exciting interface is specified externally. All the considerations on the regime of differentiating circuit remain in place. Obviously, in this setting, the fast transmitted signal (below, the ε response) is proportional to the permittivity. A calibration of the system for quantitative measures is easily

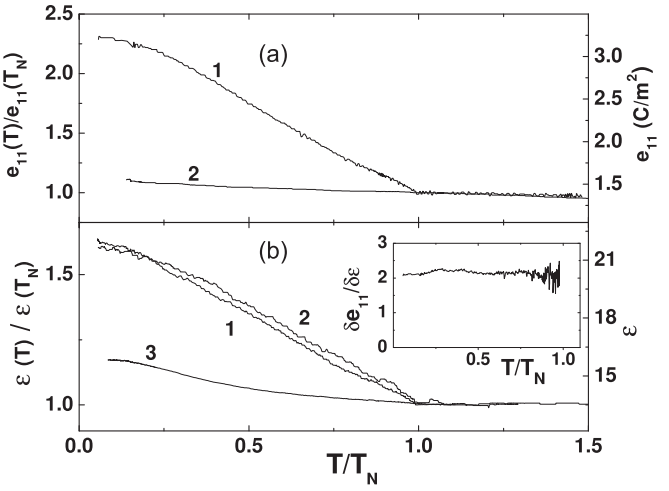

FIG. 1. Temperature variations of electrical parameters for studied ferroborates in a magnetically ordered phase. (a) Change of piezomoduli in samarium (1) and neodymium (2) ferroborates (H=0). (b) Change of permittivity in $SmFe_3(BO_3)_4$: **E**‖**x**, H=0 (1), **E**‖**y**, H=0 (2), **E**‖**x**, H=2.5 T (**H**‖[110]) (3). Inset: the temperature behavior of the ratio of relative changes in the dielectric constant and piezoelectric coefficient (H=0).

performed by replacing the sample with a known capacity of nearly the same magnitude. This approach avoids the problems of accounting the matching quality of the receiving feeder. We note that in the ε experiment as well as in the p experiment with piezoelectric materials the energy is transmitted to the receiving interface via two channels, albeit with a different ratio of the amplitudes of the fast and slow components. In our experiments, due to the use of sufficiently thick samples (~2 mm) and the time of flight technique, it was possible to distinguish the contribution of these components. Actually, in the ε experiment, the slow component does not exceed the level of a few percent of the fast one. But at lower frequencies, we fall into an area of piezoelectric resonances [7], where the acoustic channel gives the principal contribution (2–10 MHz for our samples). Unfortunately, the available sizes of the samples under investigation do not allow realizing the time of flight regime at such low frequencies and differentiation of these contributions requires a different approach.

In Fig. 1(a), we present the results of p experiments for the longitudinal wave propagating along the piezoactive **x** direction in the absence of the magnetic field. In $NdFe_3(BO_3)_4$, the influence of the magnetic ordering on PM is negligible. In the samarium compound below the Neel temperature, a significant increase of the p response is observed, which is quite unusual for an improper ferroelectric. By the form of the temperature dependence and the scale of the effect, the phenomenon is similar to the behavior of the permittivity in $SmFe_3(BO_3)_4$ observed in Ref. [5]. Therefore we present the results of our own high-frequency ε experiments in samarium ferroborate [Fig. 1(b)]. The growth of permittivity below the Neel temperature in the absence of the magnetic field is sufficiently great, but it is about two times lower than reported in Ref. [5] at low frequencies. The assumption on the decrease of the ε response already at the frequencies used

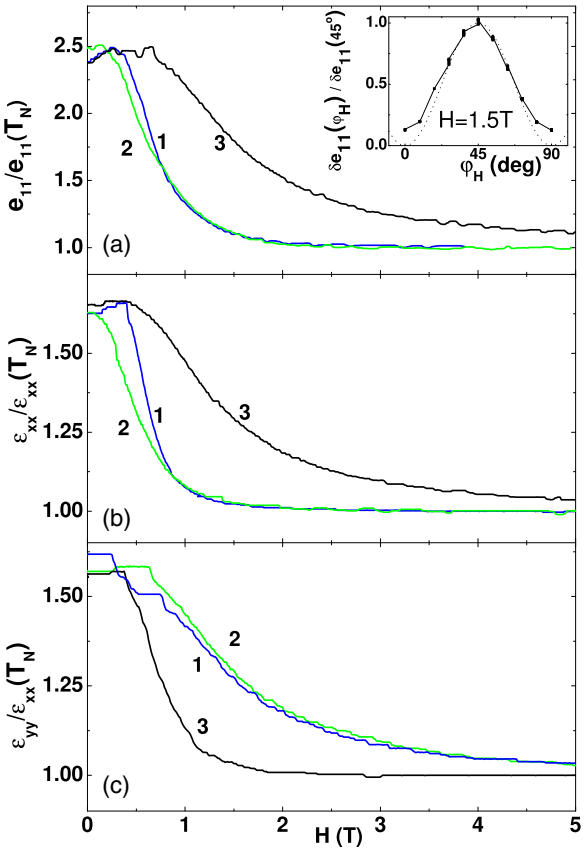

FIG. 2. (Color online) Magnetic field dependencies of p and ε responses. $T = 1.7$ K, $\mathbf{H}\|\mathbf{x}$ (1), $\mathbf{H}\|\mathbf{y}$ (2), $\mathbf{H}\|[110]$ (3). (a) Piezomodulus, inset: angle dependence of relative changes in piezoresponse, experimental data (solid line), $\sin^2(2\varphi_H)$ (dashed line). (b) Permittivity $\mathbf{E}\|\mathbf{x}$ and (c) permittivity, $\mathbf{E}\|\mathbf{y}$.

in our experiments has not been confirmed. The increase of the operating frequency up to 250 MHz results even in a small growth of the changes of ε ($\sim$20%). The reason for this discrepancy with the results of Ref. [5] is unclear. Note the absence of a noticeable anisotropy under the reorientation of the field direction between **x** and **y** axes.

The behavior of responses in both experiments in the magnetic field at $T = 1.7$ K is shown in Fig. 2. In certain directions of the field, the recorded values return to the paraelectric phase values already in the field of $\sim$2 T, but there are directions where 5 T is not enough to suppress the influence of antiferromagnetism. The obvious similarity of the results of different experiments, their pronounced anisotropy, and diametrically opposite behavior under changes of the direction of the electric field [Figs. 2(b) and 2(c)] attract the attention. In the paraelectric phase, the magnetic field of any orientation does not change the p and ε responses. The field, oriented along the **z** axis, has practically no effect on the p response.

We also note that the values given in Fig. 1 are not strictly defined—even in the same sample, the results for different cooling cycles vary in value by 10%–15% with a good reproducibility of the temperature dependencies. One might think that this variability appears due to an incomplete reproducibility of details of the domain structure.

III. DISCUSSION OF THE RESULTS

Let us give a phenomenological interpretation of the results of the performed experiments. First of all, we note that the frequency used is small compared to the characteristic energies of the excitation spectrum of the antiferromagnet, so that at any time the system is in the equilibrium (stationary) state. Therefore we can use a purely thermodynamic approach. When recording the thermodynamic potential, we believe that all material vectors have no z components. In the "elastic" part of the problem we, for simplicity, restrict ourselves to the propagation of the longitudinal sound wave along the piezoactive C_2 axis. The problem is easily solved by using strain and electric field as independent variables in the thermodynamic potential [14]. Based on the results obtained, we conclude the main contribution to the behavior of discussed characteristics comes from the magnetoanisotropic interaction.

A simple algorithm for the construction of possible invariants for a trigonal crystal using the transition to complex coordinates can be found in Ref. [13]. Eventually, taking into account the two-component order parameter for the "easy-plane" states, there exist the following invariant combinations of external fields with magnetic variables describing the interaction: (a) magnetoelectrical, $E_x(L_x^2 - L_y^2) - 2E_yL_xL_y$, and (b) magnetoelastic, $(u_{xx} - u_{yy})(L_x^2 - L_y^2) + 4u_{xy}L_xL_y$. Turning to the module of the antiferromagnetism vector L and angle φ, which determines its position in the easy-plane ($\cos\varphi = L_x/L$, $\sin\varphi = L_y/L$), we obtain

$$\tilde{F} = F_0(L^2, L_z) + K\cos 6\varphi + \frac{1}{2}C_{11}u_{xx}^2 - \frac{\varepsilon E^2}{8\pi} + e_{11}E_xu_{xx} + \frac{a}{2}(E_x\cos 2\varphi - E_y\sin 2\varphi) + \frac{b}{2}\left[\left(u_{xx} + u_{xx}^0 - u_{yy}^0\right) \times \cos 2\varphi + 4u_{xy}^0\sin 2\varphi\right] - \frac{1}{2}\mathbf{MH}. \quad (1)$$

In Eq. (1), we keep only the terms related to the experimental results obtained above (with $u_{xx} \neq 0$). The first term is the independent of φ contribution, responsible for the emergence of the "easy-plane" antiferromagnetic ordering. The second one is the anisotropy in the basal plane, the following two terms are the elastic energy and the contribution of the electric field, respectively. The next terms are the piezoelectric, magnetoelectric, and magnetoelastic contributions. The latter, besides the interaction with the elastic wave (u_{xx}), contains the interaction with the inhomogeneous static deformation (marked with the upper index "0"). The final term is the spin energy in the magnetic field. In the simplest equal-sublattice approximation of the antiferromagnet, it is equal to $\frac{1}{2}\chi H^2\sin^2(\varphi_H - \varphi)$ (χ is the magnetic susceptibility; φ_H is the angle between the direction of **H** and the **x** axis). It is assumed that all the coefficients in Eq. (1) are independent of the field variables and of φ angle, but they depend on L, and therefore on the temperature. Note that for the analysis we use the Gaussian nonrationalized system (CGS), but the final numerical values are presented in SI.

The stationary condition of the $\partial\tilde{F}/\partial\varphi = 0$ means that φ is an implicit function of the electric field and elastic deformation. Using the standard formulas $\sigma_{xx} = \frac{\partial\tilde{F}}{\partial u_{xx}} = C_{11}u_{xx} + e_{11}E_x + \frac{b}{2}\cos 2\varphi$ and $e = \partial\sigma/\partial E$ [13], for the effective PM,

we obtain

$$e_{11}^{\text{eff}} = e_{11} - b\sin 2\varphi \frac{\partial \varphi}{\partial E} = e_{11} - \frac{ab\sin^2 2\varphi}{\partial^2 \tilde{F}/\partial \varphi^2}. \quad (2)$$

To derive Eq. (2), we have used the rule of the differentiation of implicit functions. The external fields E and u can be chosen arbitrarily small, so when we find the derivative (2) they are not taken into account. This, however, does not relate to the static deformations, which, in principle, can be significant, and in some cases should be taken into account [5]. Nevertheless, at sufficiently large magnetic fields, due to the growth of the magnetic energy the second term in Eq. (2) vanishes and PM returns to its paraelectric value as follows from the experimental results. It is seen from Eq. (2) that the renormalization of the PM is indeed an indirect process. It is a joint action of the magnetoelectric and magnetoelastic mechanisms: the acoustic deformation activates the angular modulation of the antiferromagnetic vector position, resulting in the changes of the polarization and the electric field (or vice versa).

Let us now discuss the behavior of the dielectric constant. Using the equations $D = -4\pi \frac{\partial \tilde{F}}{\partial E}$ and $\varepsilon = \frac{\partial D}{\partial E}$ [13], we find that the effective permittivity coinciding with the one from Ref. [5] looks like

$$\varepsilon_{xx}^{\text{eff}} = \varepsilon_{xx} + 4\pi a \sin 2\varphi \frac{\partial \varphi}{\partial E_x} = \varepsilon_{xx} + \frac{4\pi a^2 \sin^2 2\varphi}{\partial^2 \tilde{F}/\partial \varphi^2}, \quad (3)$$

$$\varepsilon_{yy}^{\text{eff}} = \varepsilon_{xx} + 4\pi a \cos 2\varphi \frac{\partial \varphi}{\partial E_y} = \varepsilon_{xx} + \frac{4\pi a^2 \cos^2 2\varphi}{\partial^2 \tilde{F}/\partial \varphi^2}. \quad (4)$$

Thus, in the antiferromagnetic state, the crystal becomes the biaxial one. The above-mentioned absence of anisotropy of the dielectric properties with the change of the direction of the electric field [Fig. 1(b)] is explained by the averaging over the three types of domains, which arise to preserve the original trigonal macroscopic symmetry. According to (2) and (3), the behavior of e_{11}^{eff} and $\varepsilon_{xx}^{\text{eff}}$ is described by similar expressions. Since in the steady state $\partial^2 \tilde{F}/\partial \varphi^2 > 0$, from the growth of e_{11}^{eff} below T_N we can conclude that the coefficients a and b have opposite signs.

In the following, we will operate with the relative variations of measured values: $\delta e_{11}(T) = (e_{11}^{\text{eff}}(T) - e_{11}(T_N))/e_{11}(T_N)$ and $\delta \varepsilon_{xx}(T) = (\varepsilon_{xx}^{\text{eff}}(T) - \varepsilon_{xx}(T_N))/\varepsilon_{xx}(T_N)$. In terms of those variations, the ratio between coefficients a and b has the form

$$\delta e_{11}(T)/\delta \varepsilon_{xx}(T) = -b\varepsilon_{xx}(T_N)/4\pi a e_{11}(T_N), \quad (5)$$

From the form of the temperature dependencies presented in Fig. 1, it follows that the constants a and b vary with temperature by a similar manner so that their ratio is practically temperature independent [Fig. 1(b), the inset]. The change of the dielectric constant under the influence of the magnetic field is called magnetodielectric effect or magnetocapacitance. The behavior of the piezoelectric response described above can be similarly defined as the magnetopiezoelectric effect. Do not confuse it with the piezomagnetoelectric effect [15,16]. The latter corresponds to the term $E_l H_m u_{ik}$ in the thermodynamic potential and provides the direct contribution of magnetic variables to the piezoelectric response. This interaction is forbidden for the magnetic point group $21'$ to which the Sm compound belongs [16]. However, from the symmetry point of view, the thermodynamic potential may contain some other terms that lead to a direct influence of the magnetic variables on the piezoelectric effect. For example, the existence of an invariant (an actual for us part) proportional to the combination $E_x u_{xx}(L_x^2 - L_y^2)$ is possible. In terms of Ref. [16], this combination could be called piezobimagnetoelectric interaction. However, the renormalization of PM in this case would be also in the limit of a large magnetic field, and it changes the sign under rotation of **H** from the **x** to **y** axes. As follows from Fig. 2(a), such a behavior is not observed.

Let us now discuss how the transformation of the electrical parameters influences the elastic modulus, which determines the behavior of the sound velocity. As before, we restrict ourselves only with the longitudinal sound propagating along the piezoactive **x** direction. In accordance with the basic equation of motion of the elasticity theory ($\rho \ddot{u}_x = \partial \sigma_{xx}/\partial x$), we calculate the term $\partial \sigma_{xx}/\partial x$:

$$\frac{\partial \sigma_{xx}}{\partial x} = C_{11}\frac{\partial u_{xx}}{\partial x} + e_{11}\frac{\partial E_x}{\partial x} - b\sin 2\varphi\left(\frac{\partial \varphi}{\partial u_{xx}}\frac{\partial u_{xx}}{\partial x} + \frac{\partial \varphi}{\partial E_x}\frac{\partial E_x}{\partial x}\right). \quad (6)$$

To exclude the electric field from Eq. (6), we use the equation of the electrical neutrality:

$$\nabla \cdot \mathbf{D} = \varepsilon\frac{\partial E_x}{\partial x} - 4\pi e_{11}\frac{\partial u_{xx}}{\partial x} + 4\pi a \sin 2\varphi\left(\frac{\partial \varphi}{\partial u_{xx}}\frac{\partial u_{xx}}{\partial x} + \frac{\partial \varphi}{\partial E_x}\frac{\partial E_x}{\partial x}\right) = 0. \quad (7)$$

As a result, we obtain

$$\frac{\partial \sigma_{xx}}{\partial x} = \left[C_{11} + \frac{4\pi\left(e_{11}^{\text{eff}}\right)^2}{\varepsilon_{xx}^{\text{eff}}} - \frac{b^2\sin^2 2\varphi}{\partial^2 \tilde{F}/\partial \varphi^2}\right]\frac{\partial u_{xx}}{\partial x}. \quad (8)$$

The combination in square brackets represents the effective elastic modulus. Two contributions are competing: the hardening due to the piezoelectric interaction and the softening due to the magnetoelasticity. In order to understand in which direction the modulus will be changed below T_N, we need to subtract its value at the transition point [$C_{11}^{\text{eff}}(T \geqslant T_N) = C_{11} + \frac{4\pi e_{11}^2}{\varepsilon_{xx}}$] [13]. As a result, the change in the sound velocity is

$$\frac{\Delta s}{s} = \frac{C_{11}^{\text{eff}}(T) - C_{11}^{\text{eff}}(T_N)}{2C_{11}^{\text{eff}}(T_N)} = -\frac{\delta \varepsilon_{xx}}{1 + \delta \varepsilon_{xx}}\left(\frac{\delta e_{11}}{\delta \varepsilon_{xx}} - 1\right)^2 \frac{2\pi e_{11}^2}{\varepsilon_{xx}\rho s_{Lx}^2}. \quad (9)$$

Here, s_{Lx} is the velocity of the longitudinal mode in the **x** direction and ρ is the density. All the factors in Eq. (9) are positive, i.e., the sound velocity in **x** direction must always decrease in all the compounds of this symmetry, at least near T_N. Figure 3 compares the dependence of the velocity expected from (9) at $H = 0$ based on the results of Fig. 1 with the experimentally measured one. We used the average value $\delta e_{11}/\delta \varepsilon_{xx} = 2.15$ [see the inset in Fig. 1(b)], $\rho = 4.5\ \text{g/cm}^3$, $s_{Lx} = 8.7\times 10^3\ \text{m/s}$ (Ref. [9]), and $e_{11} = 1.4\ \text{C/m}^2$ (Ref. [9]). Notice the good qualitative agreement between the dependencies. However, a close numerical coincidence is

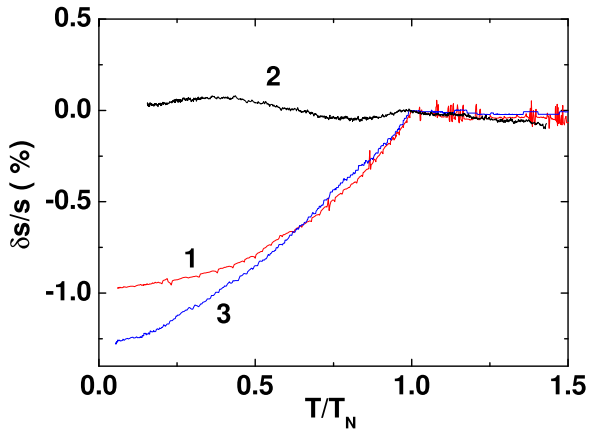

FIG. 3. (Color online) Change of the sound velocity for the longitudinal sound ($\mathbf{q} \parallel \mathbf{x}$) in the antiferromagnetic phase. $SmFe_3(BO_3)_4$ (1), $NdFe_3(BO_3)_4$ (2), calculation according to Eq. (9) for $SmFe_3(BO_3)_4$ (3).

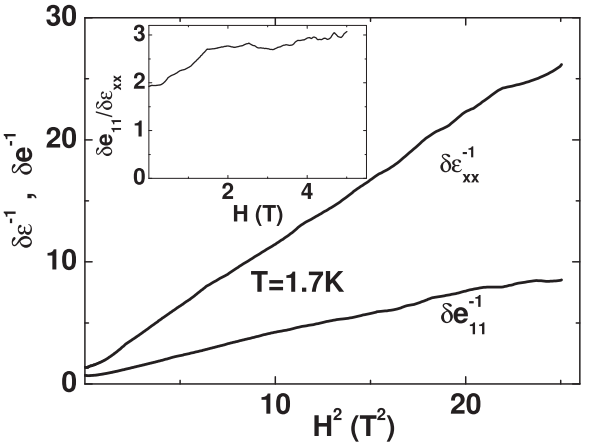

FIG. 4. Magnetic field dependencies of inverse values of relative changes of p and ε responses. In $SmFe_3(BO_3)_4$, it shows the square-law growth. (Inset) Magnetic field dependence of the ratio of discussed parameters.

probably accidental. The noted above variability of the results presented in Fig. 1 can change up to two times the value of the second factor in Eq. (9). Figure 3 shows the behavior of the sound velocity in the neodymium compound also: the magnetic ordering does not lead to any dramatic events in this case.

Magnetic field dependencies are also described by Eqs. (1)–(4). Ideally, in a single-domain crystal at $H = 0$, depending on the sign of K, the vector $\mathbf{L}$ is directed along the $\mathbf{x}$ or $\mathbf{y}$ axis, or along the symmetry-equivalent directions. When the magnetic field approaches the value of the spin flop H_{sf}, the vector $\mathbf{L}$ is set perpendicular to $\mathbf{H}$. As a rule it happens via a jump. If $\varphi_H \neq 0$, the electrical characteristics must show divergences associated with the zeroing of the second derivative $\partial^2 \tilde{F}/\partial\varphi^2$. In experiments, the field dependencies of e_{11} and ε sometimes displayed a small steplike feature, but any significant jumps, or, moreover, divergences were never observed. Such a situation is discussed in detail in Ref. [5]. The authors of Ref. [5] suggested that due to inhomogeneous static stress, a state in each domain corresponds to the continuous array of fields H_{sf}. It results in that under increase in the magnetic field the transition to a state with $\mathbf{L} \perp \mathbf{H}$ becomes a smooth one. We do not in any way object to that interpretation. Moreover, as was revealed in our work [9], the samples having a common origin with those studied in Ref. [5] show a strong inhomogeneity. However, we would like to note that the thermodynamic potential in the form of (1) and the subsequent equations belong exclusively to the single domain state. Their application to the polydomain sample by a simple algebraic summation of the contributions of individual domains is possible only in the absence of interdomain interactions (appearing, for example, due to the contribution of long-range strain fields). Otherwise, cross terms depending on the state of all domains appear in the denominator of (2)–(4). It is not at all obvious that the divergent solution will be retained.

Anyway, a detailed interpretation of the behavior of the electrical characteristics in the fields below or comparable with H_{sf} requires additional assumptions that are hardly amenable to a rigorous justification. The situation is different in fields exceeding H_{sf}—we are dealing with a single-domain sample, and all of the above formulas are applicable without any restrictions. The interpretation of the dependencies shown in Fig. 2 becomes quite transparent.

Since $H > H_{sf}$, then $\varphi \approx \varphi_H + \pi/2$, and the angular dependencies of δe_{11} and $\delta\varepsilon_{xx}$ are described by the numerator of (2)–(4), which is confirmed by the insert in Fig. 2(a). At $\varphi_H \to 0, \pi/2$ the numerator in Eqs. (2)–(4), $\sin^2 2\varphi$, approaches zero, which leads to a rapid decay of the increments of the discussed characteristics registered at those direction of the field.

However, at $\varphi_H = \pi/4$, the numerator is maximum, and the decrease of the corresponding quantities is only due to the growth of the magnetic energy. As a result, for the reciprocal value of the p response we have the expression $\delta e_{11}^{-1}(H) = \frac{e_{11}}{|ab|}(8bu_{xy}^0 + \chi_\perp H^2)$. In the discussed range of fields, the quantity $\chi_\perp$ is practically independent on field [4]; so δe_{11}^{-1} is a linear function of H^2. A similar conclusion applies to the ε response: at $E \parallel x$, we have

$$\delta\varepsilon_{xx}^{-1}(H) = \frac{\varepsilon_{xx}}{4\pi a^2}\left(8bu_{xy}^0 + \chi_\perp H^2\right).$$

Figure 4 shows the data of Fig. 2 reconstructed in accordance with this analysis. These dependencies are really close to linear ones. The relationship between these responses is still determined by the value b/a. At low fields (Fig. 4, the inset), it is close to the previously defined [Fig. 1(b), the inset], but with increasing H it increases slightly. A small displacement of the dependencies in Fig. 4 from the origin can be associated with the contribution of u_{xy}^0. At least the evaluation of this value (at known a and b, see below) gives the reasonable value $u_{xy}^0 \approx 5\times10^{-5}$.

At $\mathbf{E} \parallel \mathbf{y}$, as it follows from (4), and as are confirmed by the dependencies shown in Fig. 2(c), all the conclusions remain the same, but with the replacement of the characteristic angles, and by substituting $2(u_{xx}^0 - u_{yy}^0)$ instead of $8u_{xy}^0$.

We already know some constants in Eq. (1), e.g., $e_{11} = 1.4$ C/m^2 (Ref. [9]), $\varepsilon_{xx} = 13.5$ (Ref. [5]), and $\chi_\perp \approx 5.4\times10^{-4}$ (see Ref. [4]). The other parameters can be easily

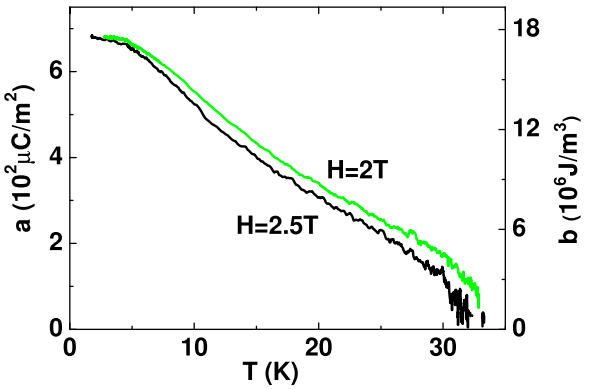

FIG. 5. (Color online) Temperature dependencies of magnetoelectric (the left scale) and magnetoelastic (the right scale) coefficients.

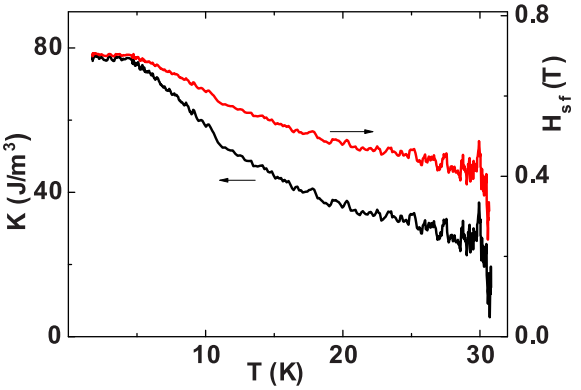

FIG. 6. (Color online) Temperature dependencies of easy-plane anisotropy parameter K_{eff} (left scale) and the calculated value of the spin-flop field H_{sf} (right scale).

estimated from the measurements in the field $\mathbf{H} \parallel [110]$ at $H > H_{\text{sf}}$. In that case, any corrections related to u^0_{xy} in $\partial^2 \tilde{F}/\partial\varphi^2$ can be neglected, and the latter is determined by the last term in Eq. (1) only.

The temperature dependence of ε response in the presence of the magnetic field [for example, the curve 2 in Fig. 1(b), measured at $H = 2.5$ T and $\varphi_H = \pi/4$] allows to determine the temperature-dependent magnetoelecric coefficient a [$4\pi a^2/\varepsilon_{xx} = \delta\varepsilon_{xx}(T,H)\,\chi_\perp H^2$]. Some of the results obtained in different magnetic fields that show the independence of a from the magnetic field are presented in Fig. 5.

The magnetoelastic coefficient b, as follows from Eq. (5) and the result presented in the inset in Fig. 1(b), coincides with a up to a scale factor. The right scale in Fig. 5 determines its value.

It is natural to assume that at $H = 0$ inhomogeneities do not violate the equivalence of all domains. In each domain, a coordinate system can be chosen such that the values of φ are the same. Then the domains will differ from each other only in the orientation of the electric field in them. To each domain corresponds one and the same effective anisotropy constant: $\partial^2 \tilde{F}/\partial\varphi^2 = 36K_{\text{eff}} = 36K + \delta K_{\text{in}}$ (δK_{in} is the contribution of the inhomogeneities). Then K_{eff} can be determined from the behavior of ε response at $H = 0$ (3): $K_{\text{eff}} = \frac{1}{2}\frac{4\pi a^2}{36\varepsilon_{xx}}\frac{1}{\delta\varepsilon_{xx}}$. The factor $\frac{1}{2}$ appeared as a result of the summation of the contributions of all domains. The dependence of K_{eff} is shown in Fig. 6. The calculated temperature dependence of the spin-flop field, obtained by using the relationship $H_{\text{sf}} \approx 6\sqrt{K_{\text{eff}}/\chi_\perp}$, is presented in the same figure.

If the estimate for u^0_{ik} given above holds, the parameter K_{eff} is determined in the main part by the average value of elastic inhomogeneities. In this case, the field H_{sf} is not associated with a specific crystallographic direction and it should be understood as an average field that creates a single-domain state with $\mathbf{L} \perp \mathbf{H}$.

Finally, the limiting calculated value of the polarization, which can be reached at $T = 2K$ in a strong field, is $P_{\text{lim}} = a/2 \approx 335$ μC/m^2. Direct static measurements give 400 μC/m^2 (see Ref. [5]) (500 μC/m^2 from Ref. [4]). The discrepancy between these values is small, but nevertheless raises questions. It is unlikely that it is due to the properties of specific samples, since in the spin-flop phase inhomogeneities should not have a noticeable effect. Apparently, there is some kind of frequency dispersion. It can be associated with sufficiently deep traps which are "invisible" in dynamic measurements.

IV. SUMMARY

The influence of the antiferromagnetic ordering on the acoustoelectrical characteristics in samarium ferroborate has been studied. A giant magnetopiezoelectrical effect, i.e., an abnormally large increase of the effective piezoelectric modulus below the Neel temperature and suppression of this growth by a magnetic field, has been discovered. It is the main result of our experiments. The origin of the effect is in the joint contribution of both magnetoelectric and magnetoelastic interactions. The evolution of this contribution in the magnetic field is caused by the growth of the magnetic energy including the spin reorientation. Ideologically, the magnetopiezoelectrical effect is similar to the magnitodielectrical effect observed earlier in Ref. [5], for which additional data on its dependence on the direction of **H** are received in the present study. Phenomenological relations that explain the behavior of the effective piezoelectric modulus and sound velocity in the antiferromagnetic phase have been obtained. It is shown that under certain experimental geometry, even in the spin-flop phase, the external fields (elastic and electric) modulate the relative orientation of the vectors **L** and **H**. Measurements in this geometry allowed us to estimate the numerical values and temperature dependencies of some phenomenological parameters that are included in the thermodynamic potential.

ACKNOWLEDGMENTS

This study was supported in part by the grants of the Russian Foundation for Basic Research 14-02-00307 and 13-02-12442 and Grant for Support of Leading Scientific Schools 924.2014.2. The authors are grateful to N.F. Kharchenko and I.E. Chupis for numerous useful discussions.

[1] D. Khomskii, Physics **2**, 20 (2009).
[2] A. P. Pyatakov and A. K. Zvezdin, Phys. Usp. **55**, 557 (2012).
[3] A. N. Vasiliev and E. A. Popova, Fiz. Nizk. Temp. **32**, 968 (2006) [Low Temp. Phys. **32**, 735 (2006)].
[4] A. M. Kadomtseva, Yu. F. Popov, G. P. Vorob'ev, A. P. Pyatakov, S. S. Krotov, K. I. Kamilov, V. Yu. Ivanov, A. A. Mukhin, A. K. Zvezdin, L. N. Bezmaternykh, I. A. Gudim, and V. L. Temerov, Fiz. Nizk. Temp. **36**, 640 (2010) [Low Temp. Phys. **36**, 511 (2010)].
[5] A. A. Mukhin, G. P. Vorob'ev, V. Yu. Ivanov, A. M. Kadomtseva, A. S. Narizhnaya, A. M. Kuz'menko, Yu. F. Popov, L. N. Bezmaternykh, and I. A. Gudim, JETP Lett. **93**, 275 (2011).
[6] R. P. Chaudhury, F. Yen, B. Lorenz, Y. Y. Sun, L. N. Bezmaternykh, V. L. Temerov, and C. W. Chu, Phys. Rev. B **80**, 104424 (2009).
[7] W. G. Cady, *Piezoelectricity: an Introduction to the Theory and Applications of Electromechanical Phenomena in Crystals*, 1st ed. (McGraw-Hill, New York, 1946).
[8] B. P. Sorokin, D. A. Glushkov, A. V. Kodyakov, L. N. Bezmaternykh, V. L. Temerov, and I. A. Gudim, Vestnik of Krasnoyarsk State University, issue 5, **49** (2004).
[9] T. N. Gaydamak, I. A. Gudim, G. A. Zvyagina, I. V. Bilich, N. G. Burma, K. R. Zhekov, and V. D. Fil, Fiz. Nizk. Temp. **41**, 792 (2015) [Low Temp. Phys. **41**, 614 (2015)].
[10] I. A. Gudim, E. V. Eremin, and V. L. Temerov, J. Cryst. Growth **312**, 2427 (2010).
[11] E. A. Masalitin, V. D. Fil, K. R. Zhekov, A. N. Zholobenko, T. V. Ignatova, and Sung-Ik Lee, Fiz. Nizk. Temp. **29**, 93 (2003) [Low Temp. Phys. **29**, 72 (2003)].
[12] D. G. Sannikov, Fiz. Tverd. Tela **4**, 1619 (1962) [Sov. Phys. Solid State **4**, 1187 (1962)].
[13] L. D. Landau and E. M. Lifshitz, *Electrodynamics of Continuous Media* (Pergamon Press, Oxford, England, 1984).
[14] The literature devoted to the consideration of ferroelectric phenomena commonly uses the polarization **P** as an independent variable, which determines the behavior of the thermodynamic potential (see, for example, Refs. [5,13]). However, in a piezoelectric, the transition from (1) to such a presentation of $\tilde{F}$ assumes an additional renormalization of the elastic moduli, which is usually omitted. In our opinion, there is no deep physical meaning of this renormalization. However, for the correct description of the behavior of the elastic characteristics, one needs to take it into account, making calculations more cumbersome. Perhaps this approach is suited for the intrinsic ferroelectric in which the polarization plays the role of the order parameter. However, for an improper ferroelectric, it is much easier to use the expansion (1).
[15] H. Grimmer, Acta Crystallogr. Sect. A **48**, 266 (1992).
[16] H. Schmid, J. Phys.: Condens. Matter **20**, 434201 (2008).